J Therm Anal Calorim (2011) 105:823–830
DOI 10.1007/s10973-011-1337-8

Utilising thermoporometry to obtain new insights into nanostructured materials

Review part 2

Joakim Riikonen · Jarno Salonen · Vesa-Pekka Lehto

ESTAC2010 Conference Special Issue

Abstract Thermoporometry is a relatively new method of characterising porous properties of nanostructured materials based on observation of solid–liquid phase transitions of materials confined in pores. It provides several advantages over the conventional characterisation methods, mercury porosimetry and gas sorption. The advantages include possibility of using short measurement times, non-toxic chemicals and wet samples. In addition, complicated sample preparation and specialised instruments are not required. Therefore, it has a great potential of becoming a widely utilised characterisation method, although its potential has not yet been widely realised. In recent years, there has been a significant increase in research activities regarding the method. In the second part of the review, results and conclusions of the recent studies about thermoporometry are surveyed and discussed focusing on the application of thermoporometry in extracting various structural information from the porous materials.

Keywords Thermoporometry · Mesoporous · Freezing · Melting · Characterisation

Introduction

Thermoporometry (TPM) is a calorimetric method of characterising properties of mesoporous materials and it is based on observation of solid–liquid phase transition in the pores. It has several advantages over the conventional characterisation methods such as short measurement times, non toxicity of the chemicals use, and usage of a common measurement instrument: differential scanning calorimeter (DSC).

In the first part of the review, thermoporometry was introduced and related results on the confinement effects on materials and solid–liquid phase transition were reviewed [1]. In the second part, the application of thermoporometry to obtain pore size distribution (PSD) and various information about the pore structure are reviewed and discussed.

J. Riikonen · V.-P. Lehto (✉)
Department of Applied Physics, University of Eastern Finland, P.O. Box 1627, 70211 Kuopio, Finland
e-mail: vesa-pekka.lehto@uef.fi

J. Salonen
Department of Physics and Astronomy, University of Turku, 20014 Turku, Finland

Calculations

Pore size dependency of melting point depression

Usually, in thermoporometry, ΔT is assumed to depend on the pore size according to Gibbs–Thomson equation

$$\Delta T = T - T_0 = -\frac{\gamma_{1s} T_0 \mathrm{d}A}{\rho \Delta h \, \mathrm{d}V} = -K\frac{\mathrm{d}A}{\mathrm{d}V} \quad (1)$$

where ΔT is the melting point depression, T_0 is the bulk melting temperature, γ_{ls} is the surface tension of liquid solid interface, ρ is the density, h is the specific enthalpy of melting, and $\mathrm{d}A/\mathrm{d}V$ is the curvature of the solid liquid interface which is $1/r$ for cylinder and $2/r$ for sphere, where r is the radius of the curvature. K is defined as $K = \gamma_{ls} T_0/\rho\Delta h$. This is slightly different approach from the method originally used by Brun et al. [2] in their influential article in which they derived their equations from Gibbs–Duhem equation. Instead of proceeding to the form of Eq. 1 they used equation

$$\frac{1}{r_s} = \frac{1}{2\gamma_{1s}} \int_{T_0}^{T} \frac{\Delta S}{v} \mathrm{d}T \quad (2)$$

where ΔS is the specific entropy change of solidification and v is the specific volume. They calculated ΔS using experimental values and were able to perform the integration in Eq. 2 without an assumption of temperature independence of $\Delta S/v$ as in Eq. 1. Value of γ_{ls} was determined using Eq. 2 and a set of samples whose pore size was measured with GS and MIP. Their result for water was $r_p = -64.67/\Delta T + 0.57$, (where r is in nm and T in K). The method used by Brun et al. is discussed in more detail by Sun and Scherer [3].

Alternative methods to establish a relation between melting/freezing and pore size based on evaluation of the free energy of the system as a function of radius of the solid core in pores have been developed by several authors [4–7]. According to these theories melting of solid inside the pores cannot happen at the equilibrium temperature due to the energy barrier caused by decrease in the radius of the solid core. It should be noted that Wallacher and Knorr considered melting to take place at equilibrium temperature owing to different pore geometry consideration [7]. These theories predict that the freezing-melting hysteresis will be decreased with decreasing pore sizes due to lowering of the energy-barrier for melting. They also predict the existence of the non-freezing δ-layer between the pore walls and the solid core and that its thickness (δ) decreases with decreasing temperature. These two predictions are in qualitative agreement with observations [8–10]. The theory by Petrov and Furó [6] was developed to arbitrarily shaped pores, although, as stated by the authors, it has limitations for very complex pore shapes. They calculated approximative melting and freezing point depressions $\Delta T_f = -K(A/V)$ and $\Delta T_m = -K(\partial A/\partial V)$ for relatively large pores, where A is the pore area and V is the pore volume. The results resemble the Gibbs–Thomson equation (Eq. 1). As stated earlier, the quantitative prediction for the melting temperature of these theories is not very accurate.

Recent article by Morishige et al. [11] provided some interesting results. In their study, they fabricated inverse carbon replicas of mesoporous SBA-15, SBA-16 and KIT-6 materials. In these inverse replicas the walls of the original materials are the pores in the inverse replica and vice versa. They also fabricated SBA-15, SBA-16, KIT-6 and MCM-41 materials with carbon modified surfaces. These samples exhibited different pore wall curvatures: positive (SBA-15, SBA-16 and MCM-41), nearly zero (KIT-6 and its inverse replica) and negative (SBA-15 and SBA-16 inverse replicas). Melting point depression was observed in all materials, although, the Gibbs–Thomson equation predicts melting point elevation for negative solid–liquid curvature. Therefore, the authors concluded that the curvature of the solid–liquid interface does not appreciably affect the melting behaviour of the confined phase. They proposed that the melting point depression is controlled by the ratio of surface area to pore volume, although, the experimental evidence was not convincing due to challenging determining the ratio from nitrogen sorption measurements.

However, the measurements by Morishige et al. [11] do not prove that the solid–liquid interface has a negative curvature in the pores with negative curvature. It is possible that the ice crystals in the pores do not take the form of the pore structure but form crystals with positive surface curvature and the remaining water coexists in liquid state. Their XRD analysis of freezing and melting of the pore water does not reveal to what extent the pore water is frozen in the samples. Therefore, it would be interesting to measure the amount of solid material in the pores with negative curvature, for example with DSC, to observe if all the water in the pores with negative curvature is in solid form (except for δ-layer).

So far the lack of well established equation relating the melting point depression to the pore size has deterred thermoporometry from becoming a standard method in determining porous properties. When Gibbs–Thomson equation is used, the temperature dependencies on the parameters in Eq. 1 should be known in the temperature range of the experiment for accurate results. The true values of these parameters such as surface tension, density and specific enthalpy of melting are challenging if not impossible to determine independently. Some studies have used the bulk values extrapolated to lower temperatures [2]. However, the confinement can have unpredictable effects, e.g., on the crystal structure, and, therefore, results might be inaccurate.

Since the correct values for Gibbs–Thomson equation are not known, it is a common procedure to calibrate the value of K in Eq. 1 by measuring the melting/freezing point depression of liquid confined in porous materials with known pore size. Surprisingly, it was found that the value of $K = 26.2$ Knm in Eq. 1, calculated using the values for bulk water at T_0, can be applied with a good accuracy for a large temperature range for water in MCM-41 and SBA-15 (note that the definition of K here and in the paper by Schreiber et al. [8] differs by factor of 2). It seems that the temperature dependencies of the individual parameters in K largely cancel each other [12–14].

It has been suggested that an empirical equation $T_f = aT_0 + b/r_p$, where a and b are calibration constants can be used for calibration [12, 13]. According to these studies with substituted benzenes and linear alkanes, the same constants a and b could be used within the same family of liquids. Various other calibration curves have

also been suggested in the literature [8, 15–20]. The calibration equations can be applied with a good accuracy within the same type of porous materials.

Determination of the thickness of δ-layer

Thickness of δ-layer is of large importance in the usage of thermoporometry. The value of δ is needed in order to calculate the radius of the pore r_p, since the Eq. 1 describes only the radius of the solid core in the pore r_s ($r_p = r_s + \delta$). This is important when pores with radius of a few nanometres are being measured. Furthermore, since the δ-layer does not participate in the phase transition, calculating pore volume from the measured melting enthalpy requires the value of δ as well.

There are several ways to measure δ. In calorimetric determination the melting enthalpy of melting/freezing in confined material (ΔH) is measured. When the pore radius, the specific melting enthalpy of the crystalline part Δh_0 and the mass of confined material m are known, δ can be calculated from the equation

$$\frac{\Delta H}{m} = \Delta h_0 \left(1 - \frac{\delta}{r_p}\right)^2 \tag{3}$$

where cylindrical pore geometry is assumed. The mass of the confined material can be determined when the liquid is added to the sample or it can be determined by drying of the sample. This value might include the mass of the bulk if the pores are overfilled. The mass of the bulk phase can be calculated from its melting enthalpy and the value of m corrected accordingly.

Another possibility is to determine δ from the melting point depression of confined material using Gibbs–Thomson equation. Assuming that the curvature of the solid liquid interface is hemispherical, the curvature of the solid–liquid interface in Eq. 1 is $\mathrm{d}A/\mathrm{d}V = 2/r_s = 2/(r_p - \delta)$, where r_s is the radius of the solid core in the pore. Consequently Gibbs–Thomson equation becomes

$$\Delta T = T - T_0 = \frac{2K}{r_p - \delta} \tag{4}$$

Typically Eq. 4 is used by plotting ΔT against r_p and fitting Eq. 4 to the data points in order to avoid prior knowledge of K.

In NMRC measurements the value of δ can be determined directly from the signal of the liquid, when the solid core has been formed in the centre of the pores. Therefore, δ can be measured at any temperature below the pore freezing temperature, and not only at pore melting or freezing temperature as in the previous two methods.

An optimization method was developed by Ishikiriyama et al. [20] in order to determine the value of K and δ simultaneously. In this method the values of K and δ were optimized until the PSD determined by TPM and GS were as similar as possible. In essence this method is a calorimetric method for determining δ combined with the determination of K and δ from Eq. 4.

Pore size distribution

When the relationship between the pore size and phase transition temperature has been established and δ is known, the heat flow curve of melting or freezing can be transformed into pore size distribution with simple steps. Firstly, the baseline should be removed. Due to a change in heat capacity during melting or freezing, a sigmoidal baseline should be employed such as applied by Sun and Scherer [3]. Secondly, the temperature axis is transformed into pore size by the equation chosen, such as Eq. 4. Third step is to transform the heat flow signal into differential pore volume. This is performed using the following equation:

$$\frac{\mathrm{d}V_p}{\mathrm{d}r_p} = \left|\frac{\mathrm{d}q}{\mathrm{d}t}\frac{\mathrm{d}t}{\mathrm{d}(\Delta T)}\frac{\mathrm{d}(\Delta T)}{\mathrm{d}r_p}\frac{1}{m\Delta h\rho}\left(\frac{r_p}{r_p - \delta}\right)^z\right| \tag{5}$$

where $\mathrm{d}q/\mathrm{d}t$ is the heat flow recorded by DSC, $\mathrm{d}t/\mathrm{d}(\Delta T)$ is the inverse heating rate, m is the mass of the dry porous material, ρ is the density of ice inside the pores, the last term in the brackets is the correction term to account for the δ-layer, and z is the shape factor, which is 1 for slit, 2 for cylindrical and 3 for spherical pore geometry. The Eq. 5 is derived from the equations presented by Landry [18] and Ishikiriyama et al. [20]. For example, if Eq. 4 is used to describe the relation between pore size and melting point depression and the pore geometry is expected to be cylindrical, Eq. 5 becomes

$$\frac{\mathrm{d}V_p}{\mathrm{d}r_p} = \left|\frac{\mathrm{d}q}{\mathrm{d}t}\frac{\mathrm{d}t}{\mathrm{d}(\Delta T)}\frac{2Dr_p^2}{m\Delta h\rho\left(r_p - \delta\right)^4}\right| \tag{6}$$

The temperature dependent values of Δh and should be used if possible. For information related to the practical aspects of the measurements the excellent paper by Landry [18] is recommended.

Applications

Pore structure determinations

Evaluation of the pore structure including shape and connectivity of the pores, and pore blocking is based on the observation of the freezing-melting hysteresis. It is not a straightforward process because the nature of the hysteresis has not been well established. It also requires prior

knowledge of the sample and is, therefore, most applicable when comparing samples that have the same type of structure.

Pore connectivity

The effect of the pore blocking on freezing and melting of confined water was reported by Morishige et al. [21]. They measured melting and freezing of water in the pores of KIT-5, which consists of spherical cavities connected through narrow necks. They concluded that when the neck size was below the critical size, the freezing in the spherical cavities took place by homogenous nucleation and a narrow exothermic peak was observed at low temperatures ($\Delta T = -41$ K) in the DSC heat flow curves. The freezing point of water in the narrow necks ($\sim$4 nm) was depressed below the homogenous nucleation temperature. Therefore, there was no ice present in the openings of the cavities to provide nucleation centres and the homogenous nucleation occurred at the homogenous nucleation temperature. The homogenous nucleation temperature in the spherical cavities was 232 K and was independent of the cavity size in the cavities between 10 and 17 nm in diameter. In the samples with the neck size large enough for the water to freeze above the homogenous nucleation temperature, the freezing behaviour was drastically changed. In these samples, freezing was initiated by nucleation at the bulk ice phase and proceeded by penetration of the ice phase through the pore network. Consequently, a broader exothermic peak associated with freezing was observed at higher temperatures and its peak temperature was dependent on the neck size. The melting temperature of ice in the samples was independent of the neck size but was found to depend on the size of the cavity (ΔT from -13 to -7 K).

Similar study on the pore blocking effects was conducted by Khokhlov et al. [22] in which they studied freezing and melting of nitrobenzene in PSi using NMRC. The PSi sample consisted of parallel cylindrical pores that were composed of two alternating sections with different pore sizes. In contrast to the results by Morishige et al., they reported size dependency of homogenous nucleation inside the pores. Nucleation occurred at 230 and 240 K in the pores with sizes 7.5 and 10.4 nm, respectively, with similar neck sizes of the narrow pores ($\sim$6 nm). The authors hypothesise that the reason for the apparently strong pore size dependency to the homogenous nucleation temperature is the strains in the PSi associated with freezing. The sample in which the homogenous nucleation occurred at 240 K contained already over 10% of frozen nitrobenzene. This amount of frozen nitrobenzene was in the large pores which had openings on the surface and could, therefore, nucleate from the solid outside the pores. No significant amount of frozen pore liquid was present in the sample where the homogenous nucleation took place at 230 K. Freezing of organic liquid in the pores is known to cause compression of the PSi lattice [23]. It has been also shown that nucleation temperature follows the pressure trend of melting; if melting point is elevated by applying pressure, also the nucleation temperature is elevated [24, 25]. Possibly, the pressure, applied to the pore liquid by the freezing of the pores connected to the surface, increased the homogenous nucleation temperature.

Pore connectivity effects on the freezing and melting of nitrobenzene in Vycor were studied by Kondrashova et al. [26]. They applied temperature programs in which the cooling or freezing scan was reversed upon incomplete melting or freezing. They observed the phase transition with NMR but similar study would be possible to conduct with DSC as well. By scanning the melting and freezing curves, they were able to reveal the complexity of the pore structure. Enlightening example was the comparison of the freezing in two samples with different histories. The freezing behaviour differed dramatically between the samples, even though; at an early point of the freezing scan the temperature and the amount of frozen phase were similar in both experiments. The difference between the histories of the samples was that the sample (i) was first completely frozen and then partially melted before the freezing scan, whereas the sample (ii) was first only partially frozen and then heated to the temperature close to the pore melting point before the freezing scan. Freezing in the sample (i) took place continuously right after the reversal of the temperature. In contrary, freezing in the sample (ii) was hindered until pore freezing temperatures (in which the liquid in the pores freezes when cooling was begun from completely liquid state). This behaviour was explained by the fact that in the sample (ii) solid state existed as a continuous phase and during cooling freezing took place by penetration of the solid front further in the pore network in similar way than it occurred when starting from completely liquid state. However, the partial melting of the sample (i) had caused the smallest pores in the pore network to melt, leaving a large number of crystals scattered in the pore network. These crystals can readily act as nucleating centres for freezing and the pore blocking effect is partially bypassed. Similar results about the different configurations of solid in partially frozen and partially molten states have been shown by NMR cryodiffusometry, where the diffusion of liquid molecules can be seen as a measure of the size of the liquid domains in the pores [27–29].

Pore shape

Pore shape has been evaluated from thermoporometry data by determining a shape factor for the pores from the hysteresis between melting and freezing [2, 3, 30, 31]. This

approach is rather problematic owing to the fact that the nature of the hysteresis is not well established and there are also other factors, such as pore blocking, affecting the hysteresis.

The determination of pore shape was already proposed by Brun et al. [2]. Their method was based on different shapes of solid–liquid interface during freezing and melting. For cylindrical pores, the shape of the interface is hemispherical during freezing, when solid front penetrates the pores and during melting the shape is cylindrical adopting the cylindrical shape of the pore. Therefore, by following the Eq. 1, the melting point depression would be $\Delta T_m = K/r_s$ and freezing point depression $\Delta T_f = 2\ K/r_s$. For spherical pores, the interface is spherical in both cases and there would be no hysteresis. Therefore, the value of $\Delta T_m/\Delta T_f$ is 1/2 and 1 for cylindrical and spherical pores, respectively. This formulation was used by Sun and Scherer [3], who developed a method to evaluate the shape of the pores as a function of frozen fraction in the pores which can be interpreted as a measure of the pore size. This kind of interpretation of hysteresis has been challenged in several studies [6, 21, 32, 33]. It is clear that this kind of pore shape analysis is not valid for small pores, since the hysteresis width decreases when the pore size decreases even in well defined cylindrical pores (see discussion in the first part of the review [1]). In addition, it is not applicable if pore blocking causes considerable effects on freezing. Pore blocking effects are most likely causing the values of $\Delta T_m/\Delta T_f$ to be under 1/2 in mortar samples of Sun and Scherer [3].

Petrov and Furó [30] have used different kind of formalism to evaluate the pore shape. Based on their free energy theory, described earlier, freezing in the pores takes place at $\Delta T_f = -K(A/V)$ and melting at $\Delta T_m = -K(\partial A/\partial V)$. Therefore, the ratio $\Delta T_m/\Delta T_f = (\partial A/\partial V)(V/A)$ is dependent on the pore shape. For the simple geometries; cylindrical and spherical, the values of $\Delta T_m/\Delta T_f$ are 1/2 and 2/3, respectively, which is different than the values according to Brun et al. [2]. It was stated by the authors that their model is not valid for small pores and in materials exhibiting pore blocking.

The authors have recently presented a report on the specific use of freezing-melting hysteresis to evaluate pore shape [34]. A unique freezing-melting hysteresis of water confined in the pores of SBA-15 was found where freezing produced a single narrow exothermic peak and melting produced two endothermic peaks (Fig. 1). The peaks were well reproducible when separate samples from the same SBA-15 batch were measured, but proportional areas of the peaks were found to be different for the different SBA-15 batches. However, similar hysteresis was not observed in GS, in which the adsorption and desorption took place in single steps. This kind of hysteresis had not been reported

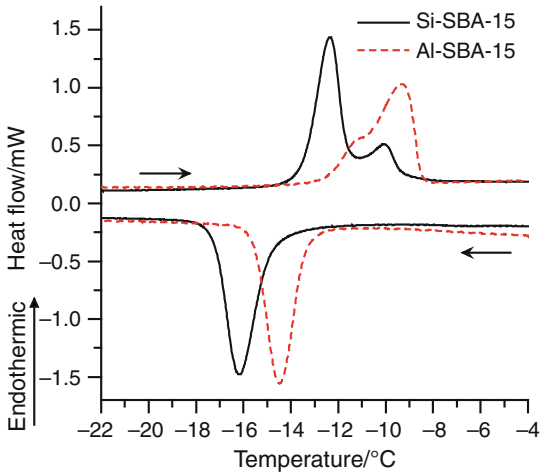

Fig. 1 Freezing and melting of water in the pores of Si-SBA-15 (*solid line*) and Al-SBA-15 (*dashed line*), showing bimodal melting peaks associated with melting in u-shaped and straight pores [34]

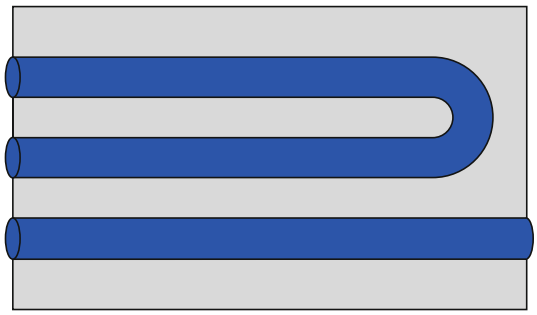

Fig. 2 Schematic figure of a u-shaped pore and straight pore in SBA-15

previously, but it was noted by Findenegg et al. [14] that water in SBA-15 typically exhibits weak anomalous broadening on the low temperature side of the melting peak which cannot be explained by the PSD of the material. Data acquired by Cides da Silva et al. [35] showed small secondary peak which is noticeable on the high temperature side of the main peak.

The authors attributed this behaviour to two types of pores in SBA-15, u-shaped and straight (Fig. 2) [36]. The tortuosity of the u-shape is potentially causing defects in the crystal structure of the water and, therefore, melting in the u-shaped pores is initiated in the tortuous part at slightly lower temperatures than in the straight parts. After melting is initiated, it proceeds through the whole pore and, therefore, the melting peak at lower temperature is not only from the tortuous part but from all the pores including u-shape. Freezing, on the other hand, is initiated at the bulk ice outside the pores and takes place at the same temperature in both types of pores. By measuring the melting enthalpies associated with the two types of pores, the fraction of pores containing the u-shapes can be calculated.

SEM imaging supported the interpretation qualitatively. The authors are not aware of any other method to perform this kind of calculation.

Studies by Huber et al. and Henschel et al. showed that a linear alkane (C19) exhibits reduced ordering in the tortuous pores of Vycor compared with the straight pores of PSi. Although, water is very different compared to a long chain linear alkane, similar reducing of ordering can take place also with water in the tortuous parts of SBA-15.

An additional implication of our interpretation of the hysteresis in SBA-15 is that the melting of water in the cylindrical, straight pores of SBA-15 does not take place at equilibrium temperature. This is because melting in the pores, including the tortuous parts, occurs at lower temperatures than melting in the pores that do not include the tortuous parts. Therefore, the equilibrium melting temperature is closer to the temperature at which water in the pores, including the tortuous parts, melts.

In conclusion of the pore structure determinations, the authors can make the following observations. If a large hysteresis between melting and freezing is observed (in the presence of solid phase outside the pores), pore blocking effects are evident. Moreover, if freezing occurs as a sharp transition ($\sim$230 K for water) it is most likely due to homogenous nucleation and the shape of the peak does not represent PSD.

Pore shape analysis should be conducted only with relatively large mesopores. In addition, the samples should exhibit a considerable pore blocking effect. The pore blocking effects should be suspected if the values of the ratio $\Delta T_m/\Delta T_f$ are smaller than 0.5.

It has been debated whether the freezing or melting transition should be applied when determining the PSD [2, 12, 18, 37]. Similarly, the use of either adsorption or desorption in GS has been argued [38]. Indeed, it has been shown that melting-freezing hysteresis is very similar to the adsorption–desorption hysteresis [39]. It is often concluded that melting transition gives more realistic presentation of the pore sizes in the sample because freezing is prone to be delayed due to the pore blocking effects [14, 21, 26]. Therefore, in general, if the "neck size" of the pores is of interest, then freezing should be employed but if the size of the cavities inside the material is of interest, then melting should be utilised. However, it should be noted that neither freezing nor melting should be blindly used for PSD calculations since melting can also exhibit anomalous behaviour as was shown to occur with u-shaped pores of SBA-15.

Studies on confined material

Thermoporometry is a method that can be used to probe the properties of the porous material, however, similar measurements and methodology can also be used to determine the properties of the material confined in the pores. For example, it is possible to predict the bulk melting points of polymorphs that are not formed under the normal conditions [40]. This can be done by measuring the melting point in various sizes of pores and extrapolating the melting point to infinitely large pores.

In drug delivery applications, it is important to know the amount of a crystalline drug in the sample. A crystalline phase is in a low energy state which has a slow dissolution rate compared to high energy disordered phase. Therefore, by inducing amorphicity in the sample the dissolution rate can be enhanced, which is desired for poorly soluble drugs. Therefore, measuring the thickness of the disordered δ-layer provides significant information about the drug loaded mesoporous material.

The authors used slightly modified version of the calorimetric method to evaluate δ [41]. The measured melting enthalpy per mass of confined ibuprofen $\Delta H/m$ was plotted versus pore radius for a series of ibuprofen loaded porous silicon samples with various pore sizes. In order to determine the value of δ, as well as Δh_0 for ibuprofen, the Eq. 3 was fitted to the data points (Fig. 3). The value of Δh_0 can be used to give an implication if the crystal structure remained unchanged due to the confinement. Moreover, from the quality of the fit, the suitability of the model geometry, crystalline core surrounded by δ-layer, was confirmed. Depending on the surface chemistry, the value of δ was between 1.2 and 2.0 nm and the value of Δh_0 was found to be close to the bulk value.

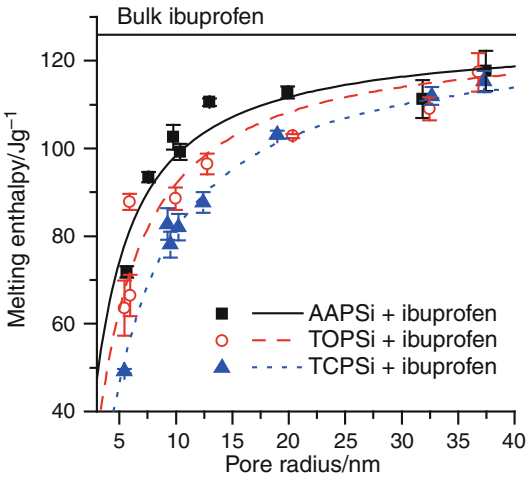

Fig. 3 Melting enthalpy of ibuprofen confined in the pores of porous silicon with various pore sizes and surface chemistries. Lines are fitted according to Eq. 3. The data points and fitted lines are grouped according to the surface treatment: as-anodized PSi (*squares* and *solid line*), thermally oxidised PSi (*circles* and *dashed line*), and thermally carbonised PSi (*triangles* and *dotted line*) [41]

It should be noted that in this method, the authors assumed δ to be independent of pore size and temperature, which is not totally valid assumption [10]. Apparently, the temperature dependency and the pore size dependency of δ partially cancelled each others. The melting enthalpy of the ibuprofen in the samples was observed at different temperatures in differently sized pores because of the pore size dependent melting temperature. The value of δ should be larger in the samples with small pore size but melting in these pores occurs at lower temperatures which decreases the value of δ. Therefore, the difference in δ is not as large at the pore melting points as it would be at a single temperature.

Quality control

Thermoporometry is especially suitable for quality control. When no detailed information on the PSD is required, experiments can be conducted with relatively high heating rates, reducing a measurement time. To demonstrate this, the authors measured freezing and melting of water inside two batches of SBA-15 with three samples from each batch with cooling/heating rate of 5 K/min (Fig. 4). The pore size was 0.26 nm larger in batch 2 than in batch 1 according to GS measurements. The differences in the freezing and melting temperatures were easily observed and the difference in the amount of the u-shaped pores was visible as well. This kind of measurement can be performed in approximately 10 min, which means a considerable increase in the throughput of samples compared to nitrogen sorption in which a measurement of one sample takes hours. Moreover, modern DSC equipment often have automatic sample changers which further increases the throughput compared to other methods.

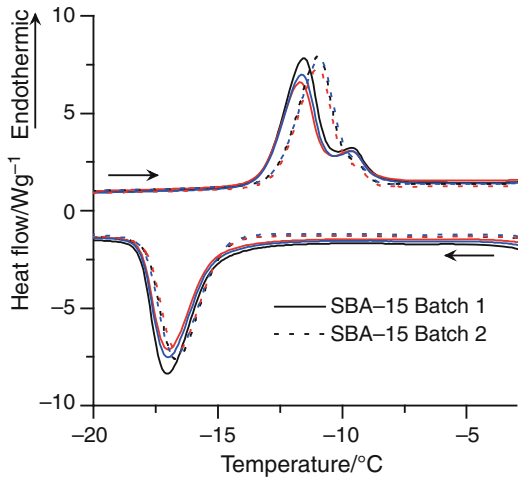

Fig. 4 Freezing and melting of water in two different SBA-15 batches; batch 1 (*solid lines*) and batch 2 (*dotted lines*), with three samples from each batch. The change in the freezing and melting temperatures due to 0.26 nm difference in the pore diameter can be observed

Conclusions

It has been shown that various information can be obtained using thermoporometry. Information about pore size, pore shape and pore structure can be obtained and with similar measurements, it is possible to study properties of confined materials themselves.

There are still many open questions in the theory of thermoporometry such as in the nature of the melting-freezing hysteresis, properties of the confined materials and even the reason for the melting point depression of confined fluids will certainly inspire numerous scientific publications. This should not, however, hinder researchers from utilising the method routinely in their studies of mesoporous materials. Similar lack in the knowledge exists also in the theories behind gas sorption methods, yet they are widely utilised.

Acknowledgements The financial support from the Academy of Finland (Grant no. 118002 and 122314) is acknowledged.

References

1. Riikonen, J, Salonen, J, Lehto, V. Utilising thermoporometry to obtain new insights into nanostructured materials—review part 1. J Therm Anal Calorim. 2010 p 97.
2. Brun M, Lallemand A, Quinson J, Eyraud C. A new method for simultaneous determination of size and shape of pores: the thermoporometry. Thermochim Acta. 1977;21:59–88.
3. Sun Z, Scherer GW. Pore size and shape in mortar by thermoporometry. Cem Concr Res. 2010;40:740–51.
4. Unruh KM, Huber TE, Huber CA. Melting and freezing behavior of indium metal in porous glasses. Phys Rev B. 1993;48:9021–7.
5. Denoyel R, Pellenq RJM. Simple phenomenological models for phase transitions in a confined geometry. 1: melting and solidification in a cylindrical pore. Langmuir. 2002;18:2710–6.
6. Petrov O, Furó I. Curvature-dependent metastability of the solid phase and the freezing-melting hysteresis in pores. Phys Rev E. 2006;73(011608–1):011608–17.
7. Wallacher D, Knorr K. Melting and freezing of ar in nanopores. Phys Rev B. 2001;63:104202.
8. Schreiber A, Ketelsen I, Findenegg GH. Melting and freezing of water in ordered mesoporous silica materials. Phys Chem Chem Phys. 2001;3:1185.
9. Morishige K, Kawano K. Freezing and melting of water in a single cylindrical pore: the pore-size dependence of freezing and melting behavior. J Chem Phys. 1999;110:4867–72.
10. Petrov OV, Vargas-Florencia D, Furó I. Surface melting of octamethylcyclotetrasiloxane confined in controlled pore glasses: curvature effects observed by ^{1}NMR. J Phys Chem B. 2007;111:1574–81.
11. Morishige K, Yasunaga H, Matsutani Y. Effect of pore shape on freezing and melting temperatures of water. J Phys Chem C. 2010;114:4028–35.

12. Billamboz N, Baba M, Grivet M, Nedelec J-. A general law for predictive use of thermoporosimetry as a tool for the determination of textural properties of divided media. J Phys Chem B. 2004;108:12032–7.
13. Bahloul N, Baba M, Nedelec J-. Universal behavior of linear alkanes in a confined medium: Toward a calibrationless use of thermoporometry. J Phys Chem B. 2005;109:16227–9.
14. Findenegg GH, Jaehnert S, Akcakayiran D, Schreiber A. Freezing and melting of water confined in silica nanopores. Chem Phys Chem. 2008;9:2651–9.
15. Jackson CL, McKenna GB. The melting behavior of organic materials confined in porous solids. J Chem Phys. 1990;93: 9002–11.
16. Wulff M. Pore size determination by thermoporometry using acetonitrile. Thermochim Acta. 2004;419:291–4.
17. Takei T, Onoda Y, Fuji M, Watanabe T, Chikazawa M. Anomalous phase transition behavior of carbon tetrachloride in silica pores. Thermochim Acta. 2000;352–353:199–204.
18. Landry MR. Thermoporometry by differential scanning calorimetry: experimental considerations and applications. Thermochim Acta. 2005;433:27.
19. Baba M, Nedelec J-, Lacoste J, Gardette J-, Morel M. Crosslinking of elastomers resulting from ageing: use of thermoporosimetry to characterise the polymeric network with n-heptane as condensate. Polym Degrad Stab. 2003;80:305–13.
20. Ishikiriyama K, Todoki M, Motomura K. Pore-size distribution (PSD) measurements of silica-gels by means of differential scanning calorimetry I. Optimization for determination of PSD. J Colloid Interface Sci. 1995;171:92.
21. Morishige K, Yasunaga H, Denoyel R, Wernert V. Pore-blocking-controlled freezing of water in cagelike pores of KIT-5. J Phys Chem C. 2007;111:9488–95.
22. Khokhlov A, Valiullin R, Kärger J, Steinbach F, Feldhoff A. Freezing and melting transitions of liquids in mesopores with ink-bottle geometry. New J Phys 2007;9.
23. Faivre C, Bellet D, Dolino G. In situ X-ray diffraction investigation of porous silicon strains induced by the freezing of a confined organic fluid. Eur Phys J B. 2000;16:447–54.
24. Yoon W, Paik JS, Lacourt D, Perepezko JH. The effect of pressure on phase selection during nucleation in undercooled bismuth. J Appl Phys. 1986;60:3489–94.
25. Yoon W, Perepezko JH. The effect of pressure on metastable phase formation in the undercooled bi-sn system. J Mater Sci. 1988;23:4300–6.
26. Kondrashova D, Reichenbach C, Valiullin R. Probing pore connectivity in random porous materials by scanning freezing and melting experiments. Langmuir. 2010;26:6380–5.
27. Dvoyashkin M, Khokhlov A, Valiullin R, Kärger J. Freezing of fluids in disordered mesopores. J Chem Phys. 2008;129.
28. Perkins EL, Lowe JP, Edler KJ, Tanko N, Rigby SP. Determination of the percolation properties and pore connectivity for mesoporous solids using NMR cryodiffusometry. Chem Eng Sci. 2008;63:1929–40.
29. Filippov AV, Skirda VD. An investigation of the structure of a porous substance by NMR cryodiffusometry. Colloid J. 2000;62: 759–64.
30. Petrov OV, Furó I. A joint use of melting and freezing data in NMR cryoporometry. Micropor Mesopor Mat. 2010;136:83–91.
31. Faivre C, Bellet D, Dolino G. Phase transitions of fluids confined in porous silicon: a differential calorimetry investigation. Eur Phys J B. 1999;7:19–36.
32. Jähnert S, Vaca Chávez F, Schaumann GE, Schreiber A, Schönhoff M, Findenegg GH. Melting and freezing of water in cylindrical silica nanopores. Phys Chem Chem Phys. 2008;10: 6039–51.
33. Morishige K, Iwasaki H. X-ray study of freezing and melting of water confined within SBA-15. Langmuir. 2003;19:2808–11.
34. Riikonen J, Salonen J, Kemell M, Kumar N, Murzin DY, Ritala M, Lehto V. A novel method of quantifying the u-shaped pores in SBA-15. J Phys Chem C. 2009;113:20349–54.
35. Cides Da Silva LC, Araújo GLB, Segismundo NR, Moscardini EF, Mercuri LP, Cosentino IC, Fantini MCA, Matos JR. DSC estimation of structural and textural parameters of SBA-15 silica using water probe. J Therm Anal Calorim. 2009;97:701–4.
36. Che SN, Lund K, Tatsumi T, Iijima S, Joo SH, Ryoo R, Terasaki O. Direct observation of 3D mesoporous structure by scanning electron microscopy (SEM): SBA-15 silica and CMK-5 carbon. Angew Chem Int Ed Engl. 2003;42:2182–5.
37. Ishikiriyama K, Todoki M. Pore-size distribution measurements of silica-gels by means of differential scanning calorimetry II. Thermoporosimetry. J Colloid Interface Sci. 1995;171:103–11.
38. Sing K. The use of nitrogen adsorption for the characterisation of porous materials. Colloids Surf A. 2001;187–188:3–9.
39. Beurroies I, Denoyel R, Llewellyn P, Rouquerol J. A comparison between melting-solidification and capillary condensation hysteresis in mesoporous materials: application to the interpretation of thermoporometry data. Thermochim Acta. 2004;421:11–8.
40. Ha JM, Hamilton BD, Hillmyer MA, Ward MD. Phase behavior and polymorphism of organic crystals confined within nanoscale chambers. Cryst Growth Des. 2009;9:4766–77.
41. Riikonen J, Mäkilä E, Salonen J, Lehto V. Determination of physical state of drug molecules in mesoporous silicon with different surface chemistries. Langmuir. 2009;25:6137–42.